Distribution of energy-momentum tensor around static quarks in SU(3) gauge theory at high temperature

Enkhtuya Galsandorj, Sodbileg Chagdaa, Battogtokh Purev and Munkhzaya Batgerel

Laboratory of Theoretical and High Energy Physics, Institute of Physics and Technology, Mongolian Academy of Sciences, Mongolia

Universität Bielefeld

CRC-TR 211 Strong-interaction matter under extreme conditions

Abstract

In this study, we explore the distribution of energy-momentum tensor around the static quark and antiquark in SU(3) pure gauge theory at finite temperature. Double extrapolated transverse distributions on mid-plane of the flux tube have been presented for the first time at nonzero temperature. Also, we investigate the spatial distributions of the flux tube on the source plane obtaining from the stress tensor for several $q\bar{q}$ separations and temperatures above and below the critical temperature. The resultant distributions show the detailed structure of the flux tube. Finally, we show the dependence of F_{stress} that is computed from the integral of the stress tensor on the distance between the quark and antiquark on a finer lattice.

Introduction

In QCD, the study of thermodynamic quantities, such as, energy density (ε), pressure (p), etc., at high temperature is important to

- describe quark confinement phenomenon,
- study state of quark gluon plasma,
- understand physics of particles from relativistic heavy-ion collision.

The most convenient method to study these thermodynamic quantities is to formulate the **energy-momentum tensor (EMT)**. Also, the energy-momentum tensor is suitable to investigate the local properties of the field in the gauge invariant manner. The EMT is four times four dimensional matrix and second-rank tensor quantity. Expectation values of the elements of the matrix correspond to the physical quantities. For example, $-T_{44}(x) = \varepsilon(x)$ (Energy density), $T_{\mu\nu}(x) = \sigma_{\mu\nu}(x), (\mu, \nu = 1, 2, 3)$ (Stress tensor).

The EMT consists of the gauge part and the fermionic part:

$$T_{\mu\nu}(x) = T^G_{\mu\nu}(x) + T^F_{\mu\nu}(x) \tag{1}$$

$$T^G_{\mu\nu}(x) = \frac{1}{g_0^2}\left[F^a_{\mu\rho}(x)F^a_{\nu\rho}(x) - \frac{1}{4}\delta_{\mu\nu}F^a_{\rho\sigma}(x)F^a_{\rho\sigma}(x)\right] \tag{2}$$

The direct discretization of EMT is non-trivial on the lattice:

$$T^{lat}_{\mu\nu} = F^{lat}_{\mu\rho}F^{lat}_{\nu\rho} - \frac{1}{4}\delta\mu\nu F^{lat}_{\rho\sigma}F^{lat}_{\rho\sigma} \tag{3}$$

$$\lim_{a\to 0} T^{lat}_{\mu\nu} \neq T_{\mu\nu} - \text{UV fluctuation} \tag{4}$$

Methods and simulation

Energy-momentum tensor on the lattice

The Gradient flow method is important tool to formulate the EMT on the lattice. The EMT is constructed from gauge invariant flowed operators using small-t expansion as follows, [1]

$$T_{\mu\nu}(t,x) = c_1(t)U_{\mu\nu}(t,x) + 4c_2(t)E(t,x), \tag{5}$$

$$U_{\mu\nu}(t,x) = G^a_{\mu\rho}(t,x)G^a_{\nu\rho}(t,x) - \frac{1}{4}G^a_{\rho\sigma}(t,x)G^a_{\rho\sigma}(t,x), \tag{6}$$

$$E(t,x) = \frac{1}{4}G^a_{\rho\sigma}(t,x)G_{\rho\sigma}. \tag{7}$$

Here $c_1(t)$ and $c_2(t)$ are flow-time dependent, two-loop order perturbation coefficents [2, 3]. Then, one can obtain the renormalized EMT by taking the zero-flow time limit,

$$T^R_{\mu\nu}(x) = \lim_{t\to 0} T_{\mu\nu}(t,x). \tag{8}$$

Energy-momentum tensor around the quark and antiquark

In the $q\bar{q}$ system, the distribution of EMT is computed from the correlation function of the EMT and Polaykov loops as follows [4],

$$\langle T_{\mu\nu}(t,x)\rangle^{lat}_{q\bar{q}} = \frac{\langle T_{\mu\nu}(t,x)\mathbf{Tr}\left[L^\dagger(0)L(R)\right]\rangle}{\mathbf{Tr}\left[L^\dagger(0)L(R)\right]} - \langle T_{\mu\nu}(t,x)\rangle. \tag{9}$$

The Polyakov loops $L(\mathbf{x})$ represent positions of a quark and an antiquark located at spatial coordinate $\mathbf{x}$.

We measured not only the EMT, but also the Polyakov loops at nonzero flow time values.

Simulation parameters

T/T_c	$N_\sigma^3 \times N_\tau$	tT^2	a, fm	R, fm	N_{conf}
0.95	$32^3 \times 8$	0.003 - 0.007	0.086	0.5 - 1.2	1000
	$48^3 \times 12$	0.003 - 0.007	0.058	0.5 - 0.9	1000
	$64^3 \times 16$	0.003 - 0.007	0.044	0.5 - 0.9	500
	$96^3 \times 20$	0.003 - 0.007	0.035	0.5 - 0.8	250
1.44	$32^3 \times 8$	0.005 - 0.014	0.057	0.5 - 0.9	1000
	$48^3 \times 12$	0.005 - 0.014	0.038	0.5 - 0.8	1000
	$64^3 \times 16$	0.005 - 0.014	0.029	0.5 - 0.6	500
	$96^3 \times 20$	0.005 - 0.014	0.029	0.4 - 0.6	250

Cylindrical coordinate

In order to study transverse distribution of the EMT on the mid-plane of the flux tube, one needs to transfer into the cylindrical coordinate system:

$$T_{\gamma\gamma'} = (e_\gamma)_\mu T_{\mu\nu}(e_{\gamma'})_\nu, (\gamma\gamma' = r, \theta, z) \tag{10}$$

$$r = \sqrt{x^2+y^2}, \theta = \tan^{-1}\left(\frac{y}{x}\right), z = z$$

$$T_{\gamma\gamma'}(r) = diag(T_{44}(r), T_{rr}(r), T_{\theta\theta}(r), T_{zz}(r)) \tag{11}$$

Double extrapolation $(a,t) \to (0,0)$

With the aim of extracting renormalized EMT, the continuum limit and the zero-t limit are taken.

1. Continuum limit $(a \to 0)$, $T = \dfrac{1}{a(\beta)\cdot N_\tau} \longrightarrow 1/N_\tau^2 = (a(\beta)T)^2$
2. Zero flow time limit $(t \to 0)$, $tT^2 \to 0$
   a. Temperature: $T/T_c = 0.95, T/T_c = 1.44$,
   b. $q\bar{q}$ separation: $R = 0.5$ fm, $R = 0.7$ fm,
   c. tT^2 =0.003-0.014, $\dfrac{1}{N_\tau} \lesssim \sqrt{8tT} \lesssim \dfrac{RT}{3}$

References

[1] H. Suzuki, PTEP 2013, 8, 083B03 (2013).

[2] R. V. Harlander, Y. Kluth and F. Lange, Eur. Phys. J. C78, 11, 944 (2018).

[3] T. Iritani, M. Kitazawa, H. Suzuki and H. Takaura, PTEP 2019, 2, 023B02 (2019).

[4] R. Yanagihara, T. Iritani, M. Kitazawa, M. Asakawa and T. Hatsuda, PoS(Lattice 2019) (2019).

[5] R. Yanagihara, T. Iritani, M. Kitazawa, M. Asakawa and T. Hatsuda, Phys. Lett. B789, 2010-214 (2019).

[6] M. Kitazawa, T. Iritani, M. Asakawa, T. Hatsuda and H. Hiroshi, Phys. Rev. D 94, 114512 (2016).

[7] C. Schlichter, G.S.Bali and K. Schilling, Nucl. Phys. B 42 273 (1995).

[8] J.R. Clem, J. Low Temp. Phys. 18 427 (1975).

Results

Stress distribution around the quark and antiquark on the source plane (z, y)

$$T_{\mu\nu}n^{(k)}_\nu = \lambda_k n^{(k)}_\mu, (k = 1, 2, 3)[5] \tag{12}$$

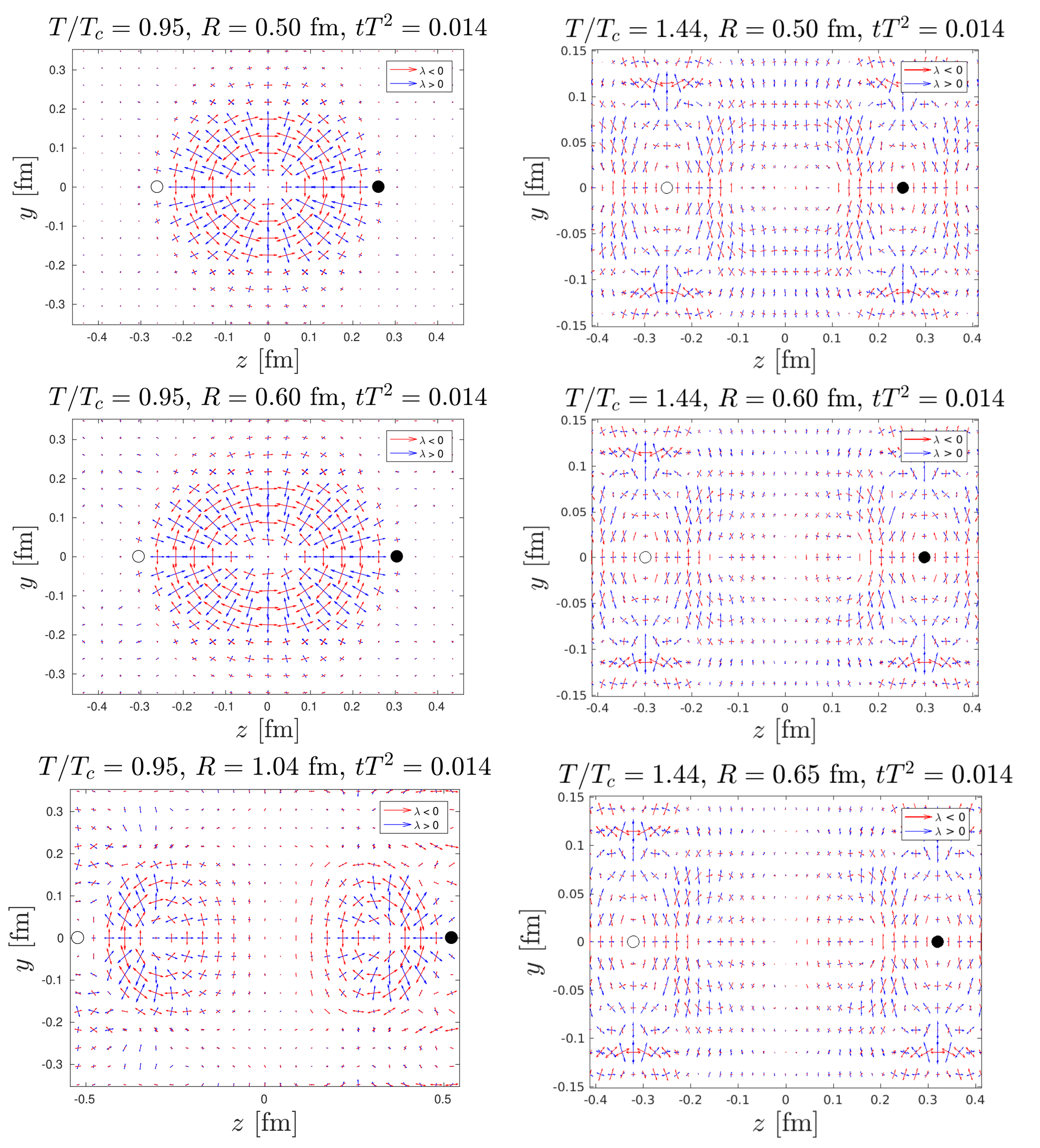

- *The shorter distance:* At both temperatures, the flux tube can be observed, but field lines are different.
- *The middle distance:* At $T < T_c$, the flux tube still persists, and at $T > T_c$, the flux tube is beginning to dissociate from the middle
- *The larger distance:* At both temperatures, the flux tube completely disappeared. But the disappearance behaviors are different.

Double extrapolation

Continuum limit $(a \to 0)$
$\langle T_{\mu\nu}(t,x)\rangle_{lat} = \langle T_{\mu\nu}(t,x)\rangle_{cont} + \dfrac{b_{\mu\nu}(t)}{N_\tau^2}$ [6]

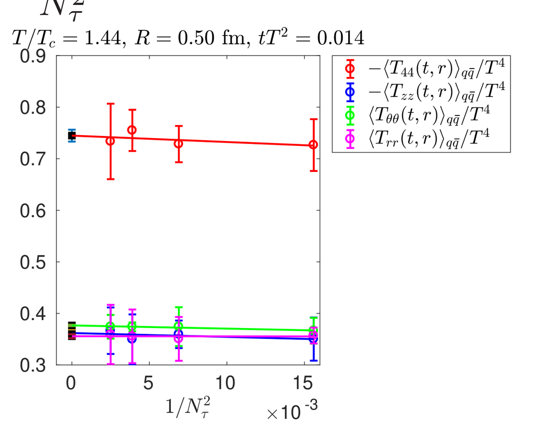

Zero-flow time limit$(t \to 0)$
$\langle T_{\mu\nu}(t,x)\rangle_{cont} = \langle T^R_{\mu\nu}(x)\rangle + C_{\mu\nu}(t)\cdot t$ [6]

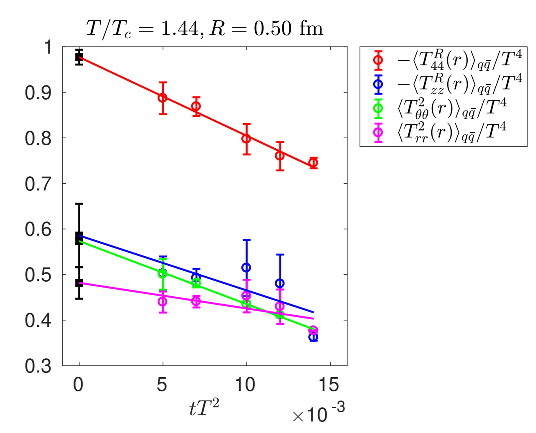

In order to parametrize the transverse profile, we have used these functions:

Gauss function:
$F_{Gauss} = A\cdot e^{-Br^2} + C$ [7]

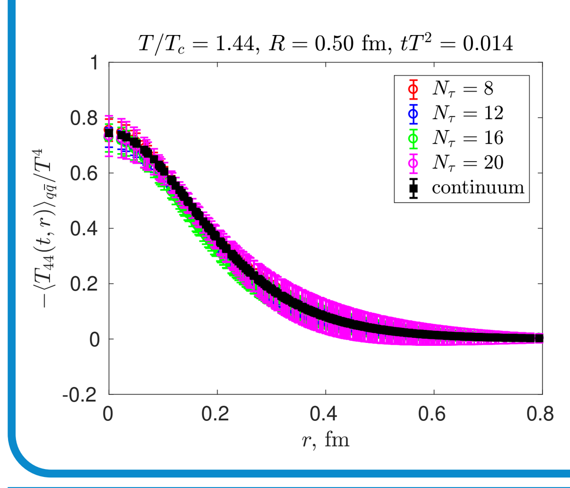

Bessel function:
$F_{Bessel} = A\cdot K_0(\sqrt{Br^2+C})$ [8]

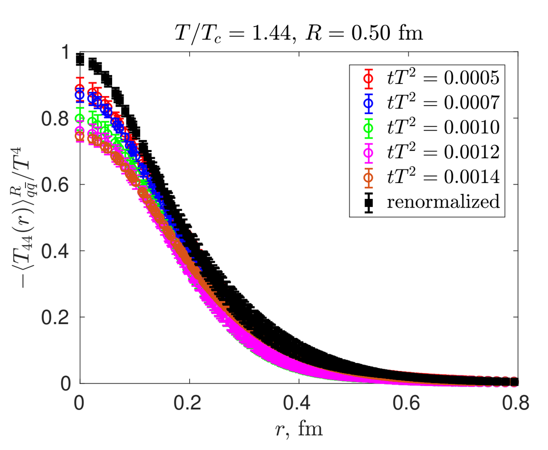

Acknowledgement

This work was carried out under the project number ShuSS-2020/24 in Mongolia. The authors thank Bielefeld's colleagues for the encouragement developing of our branch program using the SIMULATeQCD program. For coarser two lattices, generation of the gauge and flowed configurations, and flux tube measurements have been performed at the Institute of Physics and Technology of Mongolian Academy of Sciences. For two finer lattices, the simulations have been performed on the Bielefeld GPU cluster.

Results

Double extrapolated EMT distribution on midplane $(z = 0, r)$

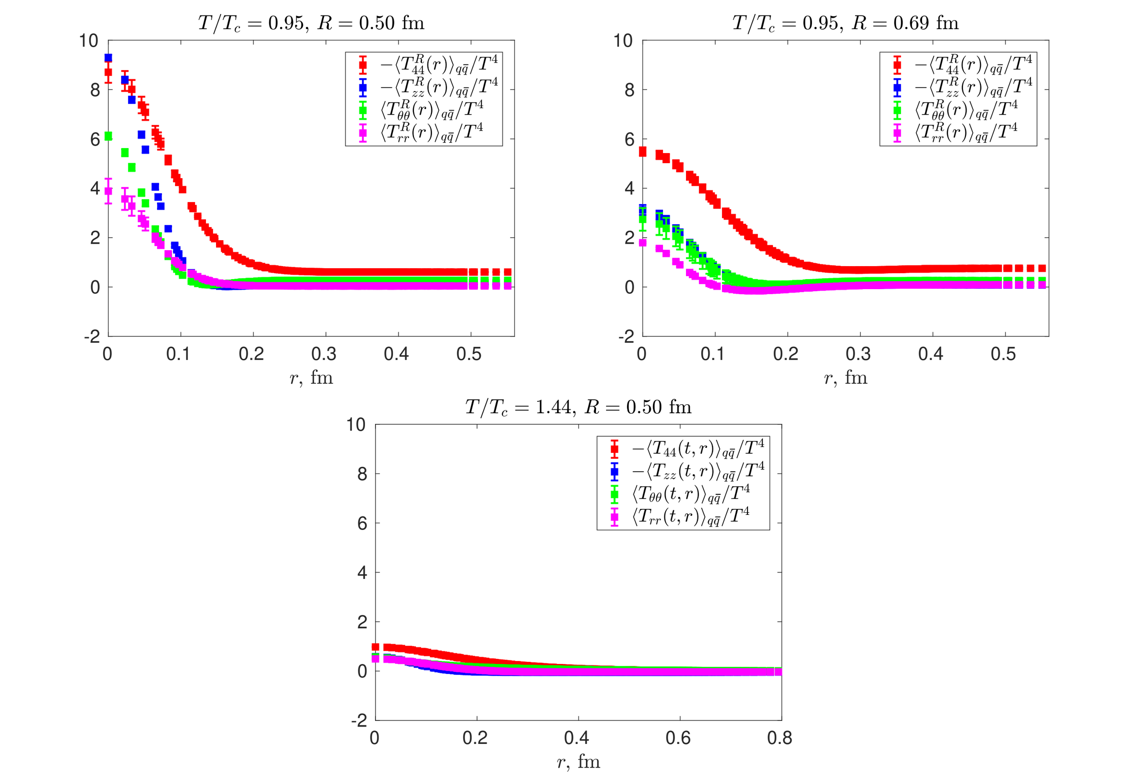

- At $T < T_c$ and for the shorter distance: The $T^R_{zz}(r)$ component, along axis connecting quarks, is larger than other two space-space components and similar to the energy density.
- For the larger distance, the $T^R_{zz}(r)$ is decreased and similar to the other two space-space components. When the distance is increased, the values of all components are decreased.
- When the temperature is increased, the values of all components are decreased and approach zero. Also, the difference between the energy density and the space-space components is decreased.

$q\bar{q}$ force computed from stress distribution

$$F_{stress} = -\int_S T_{\mu\nu}dS_j = 2\pi\int_0^\infty T_{zz}(r,t)rdr[5] \tag{13}$$

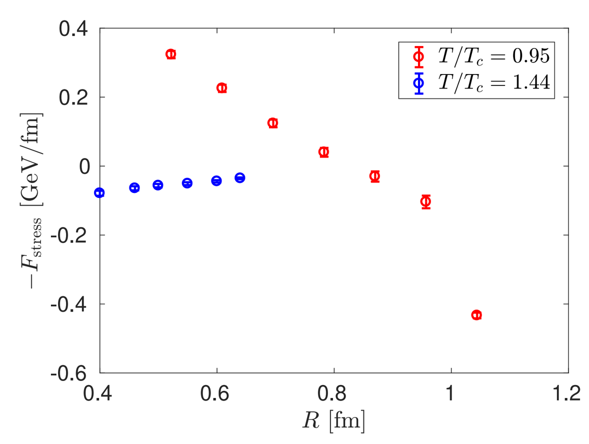

- For the temperature below T_c, the dependence of the $q\bar{q}$ force on temperature is similar to that of the zero temperature QCD, but the magnitude of the force is less than that of the $T = 0$.
- For the temperature above T_c, the dependence of the $q\bar{q}$ force on temperature is different from that of the zero temperature QCD, and it is approaching a zero. It may indicate the color screening phenomenon.

Conclusion

We have studied the distribution of the energy-momentum tensor around the quark and antiquark at high temperature in the SU(3) pure gauge theory. And we have taken the continuum limit and zero-flow time limit for the transverse profile on the mid-plane of the flux tube for the first time at nonzero temperature, successively.

- We explicitly illustrate the dissociation of the flux tube at large separation is in a different way for the temperatures below and above critical temperature from stress-tensor distribution on the source plane. This may indicate that the following phenomena are occurring:
  - $T < T_c$: String breaking
  - $T > T_c$: Color screening
- As T and R are increased: the change of the $T^R_{zz}(r)$ behavior and the decrease of all components and show the flux tube disappearance.
- $T < T_c$: $\langle T^R_{44}(r)\rangle + \langle T^R_{zz}(r)\rangle + \langle T^R_{\theta\theta}(r)\rangle + \langle T^R_{rr}(r)\rangle < 0$: similiar to the QCD vacuum and different from the classical electrodynamics.
- $T > T_c$: $\langle T^R_{44}(r)\rangle + \langle T^R_{zz}(r)\rangle + \langle T^R_{\theta\theta}(r)\rangle + \langle T^R_{rr}(r)\rangle \approx 0$: different from the QCD vacuum and similar to the classical electrodynamics.